Vision Research 110 (2015) 23–33

Contents lists available at ScienceDirect

Vision Research

journal homepage: www.elsevier.com/locate/visres

The kinetics of regeneration of rhodopsin under enzyme-limited availability of 11-*cis* retinoid

Trevor D. Lamb [a,*], Robert M. Corless [b], A. Demetri Pananos [b]

[a] Eccles Institute of Neuroscience, John Curtin School of Medical Research, The Australian National University, Canberra ACT 0200, Australia
[b] Department of Applied Mathematics, Western University, London, ON N6A 5B7, Canada

ARTICLE INFO

Article history:
Received 4 November 2014
Received in revised form 4 February 2015
Available online 10 March 2015

Keywords:
Rhodopsin
Opsin
Dark adaptation
Differential equation model
Rate limit
Lambert W function

ABSTRACT

In order to describe the regeneration of rhodopsin and the recovery of visual sensitivity following exposure of the eye to intense bleaching illumination, two models have been proposed, in which there is either a "resistive" or an "enzymatic" limit to the supply of retinoid. A solution has previously been derived for the resistive model, and here we derive an analytical solution for the enzymatic model and we investigate the form of this solution as a function of parameter values. We demonstrate that this enzymatic model provides a good fit to human post-bleach recovery, for four cases: for rhodopsin regeneration in normal subjects; for psychophysical scotopic dark adaptation in normal subjects; for rhodopsin regeneration and scotopic dark adaptation in *fundus albipunctatus* patients; and for cone pigment regeneration in normal subjects. Finally, we present arguments favouring the enzymatic model as the cellular basis for normal human rod and cone pigment regeneration.

1. Introduction

After a molecule of rhodopsin has been activated by light, it undergoes a slow process of regeneration back to its resting state, that involves release of the photo-isomerised all-*trans* retinaldehyde (retinal) and the binding of a new molecule of 11-*cis* retinal. The opsin protein molecule is located in the outer segment of a rod photoreceptor, whereas the 11-*cis* retinal is synthesised in an adjacent cell of the retinal pigment epithelium (RPE). As a result, during and after illumination, retinoid is trafficked between the two compartments, with "used" all-*trans* retinoid being transported to the RPE and "new" 11-*cis* retinal being transported back to the rod outer segment. For reviews of this system, see Lamb and Pugh (2004); Lamb and Pugh (2006) and Kiser, Golczak, and Palczewski (2013).

The time-course of regeneration of rhodopsin can be monitored spectrophotometrically; unbleached rhodopsin absorbs maximally at around 500 nm and hence appears pink, whereas the activated metarhodopsin II absorbs in the UV and is essentially colourless; after release of all-*trans* retinal, the resulting "free opsin" is also colourless. Rhodopsin regeneration can be monitored in the living human eye by reflection densitometry, whereby a beam of light is passed in through the pupil and the light reflected back from the fundus is measured. Following exposure to very intense illumination that "bleaches" essentially all of the visual pigment, rhodopsin in the human eye is regenerated over a time-course of tens of minutes, with around 95% being regenerated in 15 min. In early work, the time-course of opsin decline (the complement of rhodopsin regeneration) was described as an exponential decay, but it subsequently became clear that the initial phase could better be described as linear ramping; see Lamb (1981), reviewed in Lamb and Pugh (2004). Unfortunately, though, the noise level in densitometric recordings is typically large, so that it is difficult to determine the time-course with precision.

The late phase of opsin decline in the living human eye can be determined indirectly, by measuring human psychophysical dark adaptation, whereby the elevation of visual threshold experienced by a subject is recorded as a function of time after cessation of exposure to intense illumination; for an extensive historical review of dark adaptation studies, see Reuter (2011). Perhaps surprisingly, the elevation of visual threshold that continues after extinction of the light is primarily caused not by the *lack* of rhodopsin available to absorb photons, but rather by the *presence* of bleached "free opsin", which very weakly mimics the photo-activated state of rhodopsin (Cornwall & Fain, 1994) and thereby generates a phenomenon comparable to light, termed "dark light", that slowly fades with time.

Over a wide range of bleaching magnitudes, the elevation of visual threshold exhibits a prominent late phase of exponential decay (Pugh, 1975; Lamb, 1981), characterised in semi-logarithmic

* Corresponding author.
E-mail addresses: Trevor.Lamb@anu.edu.au (T.D. Lamb), rcorless@uwo.ca (R.M. Corless), apananos@alumni.uwo.ca (A.D. Pananos).

http://dx.doi.org/10.1016/j.visres.2015.02.014
0042-6989/

plots (of the kind illustrated in Fig. 3) by sets of parallel straight-line decline. This phenomenon was termed the "S2" component of recovery (Lamb, 1981) on the basis that it appeared to reflect the decay of a (then unknown) "Substance 2"; this substance was subsequently identified as free opsin (Cornwall & Fain, 1994). Analysis of the dependence of the size of this component of threshold elevation on the magnitude of the bleach showed that the regeneration reaction could not simply be first-order, and that the reaction instead needed to be rate-limited; i.e. in the presence of a large amount of Substance 2 (free opsin) there was a limit to the rate at which it could be regenerated back to rhodopsin (Lamb, 1981).

To account for the observed rate-limited kinetics for the regeneration of rhodopsin, a biophysical model was proposed (Lamb & Pugh, 2004; Mahroo & Lamb, 2004), indicated "Resistive" in Fig. 1, that invoked the flow of 11-*cis* retinal down its concentration gradient, through a resistance, to opsin in the outer segments. It was postulated that the RPE/retina contained a reservoir of 11-*cis* retinal at fixed concentration (C), and that there existed a physical resistance that caused a drop in concentration upon the flow of retinoid. The limiting rate occurred when the fractional concentration of 11-*cis* retinal in the outer segments (denoted c) dropped to a low value due to the "sink" caused by recombination with a high concentration of free opsin.

For that resistive model, Lamb and Pugh (2004) and Mahroo and Lamb (2004) derived an analytical solution for the fractional level of opsin $F(t)$ remaining after a fractional bleach B as

$$F(t) = K_m W\left(\frac{B}{K_m}\exp\left(\frac{B}{K_m}\right)\exp(-kt)\right) \quad (1)$$

where W represents the principal branch of the Lambert W function (Corless et al., 1996), t is time after extinction of the bleaching exposure, k is a rate constant discussed later, and K_m is a semi-saturation constant characterising the shape of the recovery. This equation was shown to provide a good description of experimental results for rhodopsin regeneration and threshold recovery.

An alternative proposal is that the rate-limit to delivery of fresh retinoid instead results from one of the several enzyme-assisted reaction steps known to be involved in the synthesis of 11-*cis* retinal, and such an alternative possibility is indicated schematically as "Enzymatic" in Fig. 1. There is, however, no clear-cut evidence in the literature as to whether the physiological rate-limit is resistive or enzymatic in nature (see Section 4). A previous study examined the differential equations that would apply if the limit were enzymatic (Lamb & Pugh, 2006), but that study was unable to derive an analytical solution for the kinetics of the resulting regeneration of rhodopsin.

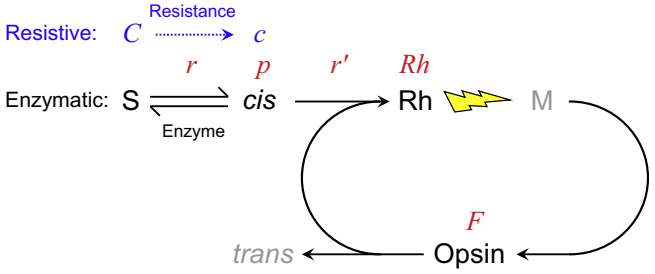

Fig. 1. Reaction schemes for resistive and enzymatic models. The opsin-rhodopsin cycle is shown at the right. Under resting dark-adapted conditions, all of the opsin has been converted to rhodopsin (Rh), which therefore has a fractional concentration $Rh = 1$. Upon illumination (jagged arrow), some fraction of rhodopsin is "bleached" to metarhodopsin (M) which decays to opsin + all-*trans* retinal (indicated "*trans*"). At our time origin of $t = 0$, all of the M has decayed, so that the fractional levels of opsin and rhodopsin are $F = B$ and $Rh = 1 - B$, where B is the fraction bleached. Thereafter, opsin combines with 11-*cis* retinal (indicated "*cis*") to regenerate rhodopsin, at a rate r' proportional to the concentrations of both reactants. In the "enzymatic" model, 11-*cis* retinal is produced from a substrate S, as the product of an enzyme-assisted reversible reaction, at a net rate r, and its fractional concentration in the photoreceptor outer segments is denoted p. For the "resistive" model, indicated in blue, 11-*cis* retinal flows at rate r down its concentration gradient, from a fixed concentration C in the RPE, through a resistive barrier, to its local concentration c adjacent to opsin in the photoreceptor outer segments. (For interpretation of the references to colour in this figure legend, the reader is referred to the web version of this article.)

In Appendix A, we derive such an analytical solution for the enzymatic model, and we investigate its dependence on values of the parameters. In Section 3 we compare the predicted solution with experimental results from the literature. Although we find that the enzymatic and resistive models are both capable of providing good fits to the experimental data, with the quality of fit being very similar in the two cases, in Section 4 we present arguments favouring the enzymatic model as the cellular basis for regeneration of rod and cone pigments.

2. Model

2.1. Description of the enzymatic model

The principal features of both the enzymatic and resistive schemes are illustrated in Fig. 1. In the resting dark-adapted state, all of the opsin has been converted to rhodopsin, giving the respective fractional levels as $F = 0$ for opsin and $Rh = 1$ for rhodopsin. Following illumination (indicated by the jagged arrow), some fraction B of the rhodopsin is bleached, and passes rapidly through the metarhodopsin state M, generating an initial opsin level of $F = B$ at our time origin of $t = 0$.

2.1.1. Binding of retinoid to opsin

Opsin then binds with 11-*cis* retinal (denoted "*cis*" in Fig. 1) to form rhodopsin once again. The local concentration of 11-*cis* retinal in the outer segment, expressed as a fraction of its resting dark-adapted level, has been denoted c in the resistive model, but in the enzymatic model is now denoted p to signify that the 11-*cis* retinal is formed as the product P of an enzymatic reaction. The rate r' of the bimolecular binding reaction is proportional to the concentrations of both reactants (11-*cis* retinal and opsin), with a bimolecular rate constant k. In darkness (and hence in the absence of any formation of opsin by illumination), r' defines the rate of decline of opsin concentration

$$r'(t) = kp(t)F(t) = -\frac{dF(t)}{dt}. \quad (2)$$

2.1.2. Retinoid supply

In both models, the rate of supply of 11-*cis* retinal is denoted r. In the resistive model, r represents the rate of flow of 11-*cis* retinal down its concentration gradient, through a resistive barrier (denoted "Resistance" in Fig. 1), from a constant concentration C in the RPE/retina to its local concentration c within the outer segments. In the enzymatic model, r represents the net rate of formation of product P by enzyme E acting on substrate S, and the concentration of this product P (i.e. 11-*cis* retinal) is denoted p, again expressed as a fraction of its resting dark-adapted level. Thus, c in the resistive model is functionally the same as p in the enzymatic model.

2.1.3. Enzymatic reaction

For the enzymatic model, the forward and reverse reactions mediated by the enzyme E have been represented schematically (see Lamb & Pugh, 2006) in the form

$$S + E \underset{k_{IS}}{\overset{k_{SI}}{\rightleftarrows}} I \cdot E \underset{k_{PI}}{\overset{k_{IP}}{\rightleftarrows}} P + E \quad (3)$$

where I is an intermediate reactant in the enzymatic conversion of the substrate S (i.e. 11-*cis* alcohol) into the product P (i.e. 11-*cis* retinal).

2.1.4. Quasi-steady state assumption

For both models, we make the quasi-steady state assumption that the rate r of supply of 11-*cis* retinal is equal to the rate r' of its binding to opsin, i.e.

$$r(t) = r'(t). \tag{4}$$

2.2. Analytical solution

In Appendix A, we derive an analytical solution for the model specified by Eqs. (2)–(4) above. Our analysis provides an inverse solution: for any desired range of values for F, in conjunction with values for the parameters, we provide an analytical solution for t. We show that the full set of parameters for the enzymatic reaction scheme can be combined to yield two non-dimensional parameters, K_1 and K_2, that specify the form of the recovery kinetics: K_1 is proportional to the total quantity of enzyme E, while K_2 specifies the relationship between product P and the proportion of enzyme E that is free for binding with substrate or product. We investigate three limiting cases (involving a total bleach, early times, and late times) and compare the predicted recovery in the enzymatic and resistive models, and thereby obtain restrictions on the ranges of K_1 and K_2 that are relevant to the living eye.

3. Results

We now compare the predictions of the enzymatic model with experimental data from human subjects, obtained using retinal densitometry and psychophysical dark adaptation for the rod system, both in normal subjects and in patients with *fundus albipunctatus*, and using ERG measurements for the cone system in normal subjects. In addition, we compare the quality of the fits obtained for the enzymatic and resistive models.

3.1. Post-bleach recovery in rods of normal human subjects

The method of retinal densitometry, for measuring the level of photopigment in the living eye, was developed in the 1950s (Campbell & Rushton, 1955). A beam of light is shone in through the pupil, and the light reflected from the fundus back out through the pupil is analysed to measure the absorption that has occurred during the presumed double-pass through the photoreceptor outer segments. In fact it is likely that much of the reflected light has not traversed the entire path both ways through the outer segments, and a detailed analysis of the likely sites of reflection and the resultant light paths has been made (van de Kraats, Berendschot, & van Norren, 1996).

Although measurements of rhodopsin content using retinal densitometry were used quite widely during the 1950s–1980s, the technique has rarely been used since that period. The measurements presented below in Fig. 2 have been taken from a study by Rushton and Powell (1972) that has been chosen as typifying the results of the technique. Recently, an alternative approach using a scanning laser ophthalmoscope has been developed (Morgan & Pugh, 2013), though to date measurements using this method have not been reported at a sufficient number of post-bleach times to render the data useful for analysis here.

Absorption measurements of rhodopsin level inevitably exhibit noise. Typically the level of such noise is substantial, which renders the method useless for small bleaches, or when regeneration is substantially complete at late times after large bleaches. For this reason an alternative approach would be very valuable. Such an alternative is in fact available from psychophysical measurements of post-bleach elevation of visual threshold, because there are strong grounds for believing that the threshold elevation measured in such psychophysical experiments is brought about by the presence of opsin that weakly mimics photo-activated rhodopsin (Cornwall & Fain, 1994) and that thereby generates a phenomenon equivalent to light, that has been termed "dark light" (reviewed in Lamb & Pugh, 2004; Reuter, 2011). The measurements presented below in Fig. 3 are from a very thorough study of psychophysical dark adaptation undertaken by Pugh (1975).

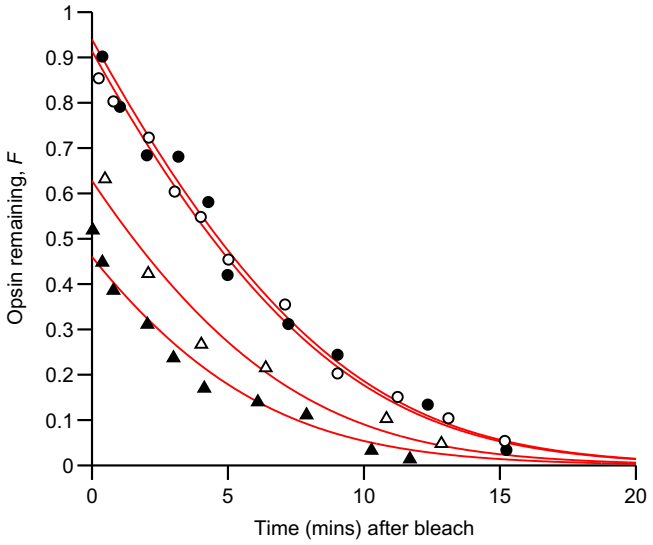

Fig. 2. Densitometric measurements of opsin decay compared with predictions of the enzymatic model. Measurements of the fraction of rhodopsin remaining unregenerated (i.e. fractional opsin, F) in the eye of a normal human subject, as a function of time after bleach extinction, from the retinal densitometry experiments of Rushton and Powell (1972). The four exposures comprised two repetitions of a near-total bleach (●, ○), and one delivery each of two smaller bleaches (△, ▲). The red traces plot the best-fitting predictions of the enzymatic model when K_2 was held fixed at $K_2 = 2$ (see Text); the values obtained for the fitted parameters were $B = 94\%$, 91%, 63%, and 46%, $K_1 = 1.55$, and $k = 0.285\ \text{min}^{-1}$, yielding an initial limiting slope for a full bleach of $v = 0.112\ \text{min}^{-1}$. The scaled residual sum-of-squares error was $SS_{\text{resid}} = 0.011$ (giving $R^2 = 0.989$). (For interpretation of the references to colour in this figure legend, the reader is referred to the web version of this article.)

3.2. Opsin decay in rods in the normal human eye from measurements using reflection densitometry

The decay of opsin level in rods measured by Rushton and Powell (1972) using retinal densitometry following bleaches of three different levels is illustrated in Fig. 2 and compared with predictions of the enzymatic model. The circles (●, ○) are for two repetitions of a large bleach, while the triangles (△, ▲) are for somewhat smaller bleaches. It is apparent from the variability of the points that there was substantial noise in the measurements.

The red curves were obtained by minimising the sum-of-squares error between the data points and the predictions of the enzymatic model, when K_2 was held fixed at $K_2 = 2$; the reason for this choice is explained below. The fitting yielded a normalised residual sum-of-squares error (see below) of $SS_{\text{resid}} = 0.011$, corresponding to a coefficient of determination of $R^2 = 0.989$. For comparison we also optimised the fit of the resistive model; the traces (not shown) were barely distinguishable by eye, and the residual sum-of-squares error was just 0.4% smaller.

3.3. Opsin decay in rods in the normal human eye from experiments using psychophysical dark adaptation

The recovery of human visual threshold, measured psychophysically by Pugh (1975) following bleaches of nine different strengths, is illustrated in Fig. 3 and compared with predictions of the enzymatic model. Each symbol type represents a separate bleach strength, ranging from 0.2% to 98% of the rhodopsin, and each plots measurements from 4 to 7 repetitions of the experimental protocol at that bleach level; inspection of the clustering for each symbol type shows that the results were quite reproducible between trials.

The red curves in Fig. 3 plot the predictions of the enzymatic model, optimised as explained below. The $\log_{10}$ threshold elevation has been calculated as $\log_{10}F + C_{\text{full}}$, where C_{full} is a constant representing the elevation of $\log_{10}$ threshold elicited by a full bleach. This logarithmic relation is expected when threshold elevation is proportional to "dark light", which is in turn proportional to opsin level, and when a full complement of opsin ($F = 1$) elevates the threshold of the rod visual system by C_{full} $\log_{10}$ units.

In fact, the experimental data are not expected to be accounted for solely by the opsin level under at least three regimes, indicated approximately by the blue lines in Fig. 3. Firstly, above the so-called "cone threshold", corresponding in these experiments to a rod threshold elevation of ~5000-fold (3.7 $\log_{10}$ units), the subject's visual threshold is determined by the cone system rather than by the rod system. Secondly, at early times during recovery, other factors such as the transient presence of metarhodopsin products are expected to induce additional threshold elevation. Thirdly, at late stages during recovery from moderate to large bleaches, additional components of "dark light" are expected to be generated, though at present these are poorly understood and have yet to be satisfactorily described. Hence, to describe the results outside the region indicated by the blue lines, factors other than opsin level alone would need to be invoked.

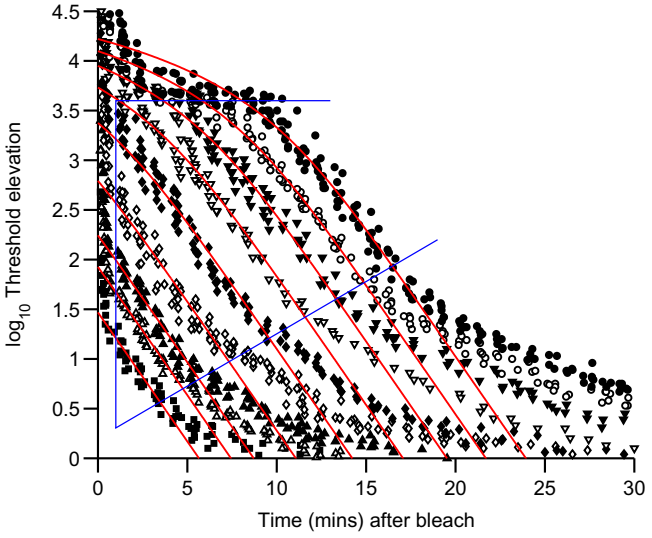

Fig. 3. Psychophysical dark adaptation recovery compared with predicted opsin decline for the enzymatic model. Recovery of $\log_{10}$ elevation of scotopic (rod) visual threshold, as a function of time after extinction of bleaching exposures. Symbols plot experimental measurements for a normal human subject made by Pugh (1975), as re-plotted in Fig. 6 of Lamb and Pugh (2004). The different symbols denote different exposure strengths, ranging from 4.7 to 7.6 $\log_{10}$ scotopic troland s. Red curves plot the predictions of the enzymatic model, with the $\log_{10}$ threshold elevation calculated as $\log_{10}F + C_{\text{full}}$. The fitting was optimised as described in the Text, with $K_2 = 2$ and with the level of the largest bleach set as 98%. The optimal fit gave $k = 0.60\ \text{min}^{-1}$ and $K_1 = 0.50$, with the vertical shift $C_{\text{full}} = 4.23$ $\log_{10}$ units; the remaining bleach levels were fitted as $B = 0.17\%$, 0.5%, 1%, 3.7%, 14%, 32%, 53%, and 74%. The blue lines indicate the region within which the experimental data points were accepted for fitting, as described in the Text. The normalised residual sum-of-squares error was $SS_{\text{resid}} = 0.0208$, giving $R^2 \approx 0.98$. (For interpretation of the references to colour in this figure legend, the reader is referred to the web version of this article.)

3.3.1. Optimisation of curve fitting

The curves shown in each of Figs. 2–5 have been optimised by minimisation of the sum-of-squares error between the data points and theory, using the "fminsearch" function in Matlab (The Mathworks, Inc.). The predictions of the enzymatic model were obtained by solving Eqs. (24) and (26). Calculations were performed in linear units for densitometry and cone measurements, and in logarithmic units for threshold measurements, i.e. as plotted in the Figures, because in those respective units the reliability of

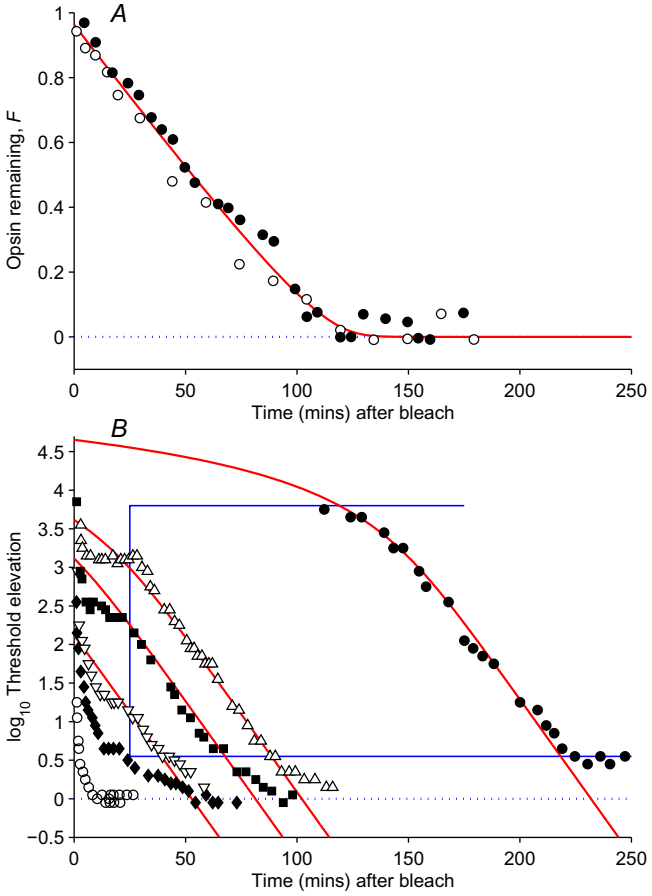

Fig. 4. Recovery of opsin level for three patients with *fundus albipunctatus*, determined from retinal densitometry (*A*) and from psychophysical dark adaptometry (*B*). *A*, Decline in opsin level determined as the complement of the rhodopsin level measured by reflection densitometry, for two brothers with *fundus albipunctatus* (●, ○), following nominally full bleaching; data from Fig. 4 of Carr, Ripps, and Siegel (1974). Red curve plots the prediction of the enzymatic model, optimised to fit the joint data for the two subjects using $K_2 = 2$, which gave $K_1 = 0.089$ and $k = 0.215\ \text{min}^{-1}$ (yielding $v \approx 0.009\ \text{min}^{-1}$) and $B = 0.96$; the normalised residual was $SS_{\text{resid}} = 0.016$ ($R^2 \approx 0.98$). *B*, Time course of decline in $\log_{10}$ threshold elevation for rod dark adaptation in a different patient, following bleaches of 0.5%, 2%, 3.5%, 6%, 12% and 99%; data from Figs. 5E and 6B of Cideciyan et al. (2000). Red curves plot the predictions of the enzymatic model, optimised using $K_2 = 2$. Blue lines indicate the region within which data points were fitted. The bleach levels B in the fitting procedure were set as the values determined by Cideciyan et al. (2000) less a fixed small amount, on the assumption (see Text) that a small residual quantity of 11-*cis* retinal was available in the outer segments; hence predictions can be made only for the four bleaching exposures that exceeded this residual level. The fitting yielded $K_1 = 0.20, k = 0.093\ \text{min}^{-1}$ (S2 slope of 0.04 decades min^{-1}), and a subtracted bleach level of 3.2%; the normalised residual was $SS_{\text{resid}} = 0.014$ ($R^2 \approx 0.99$). (For interpretation of the references to colour in this figure legend, the reader is referred to the web version of this article.)

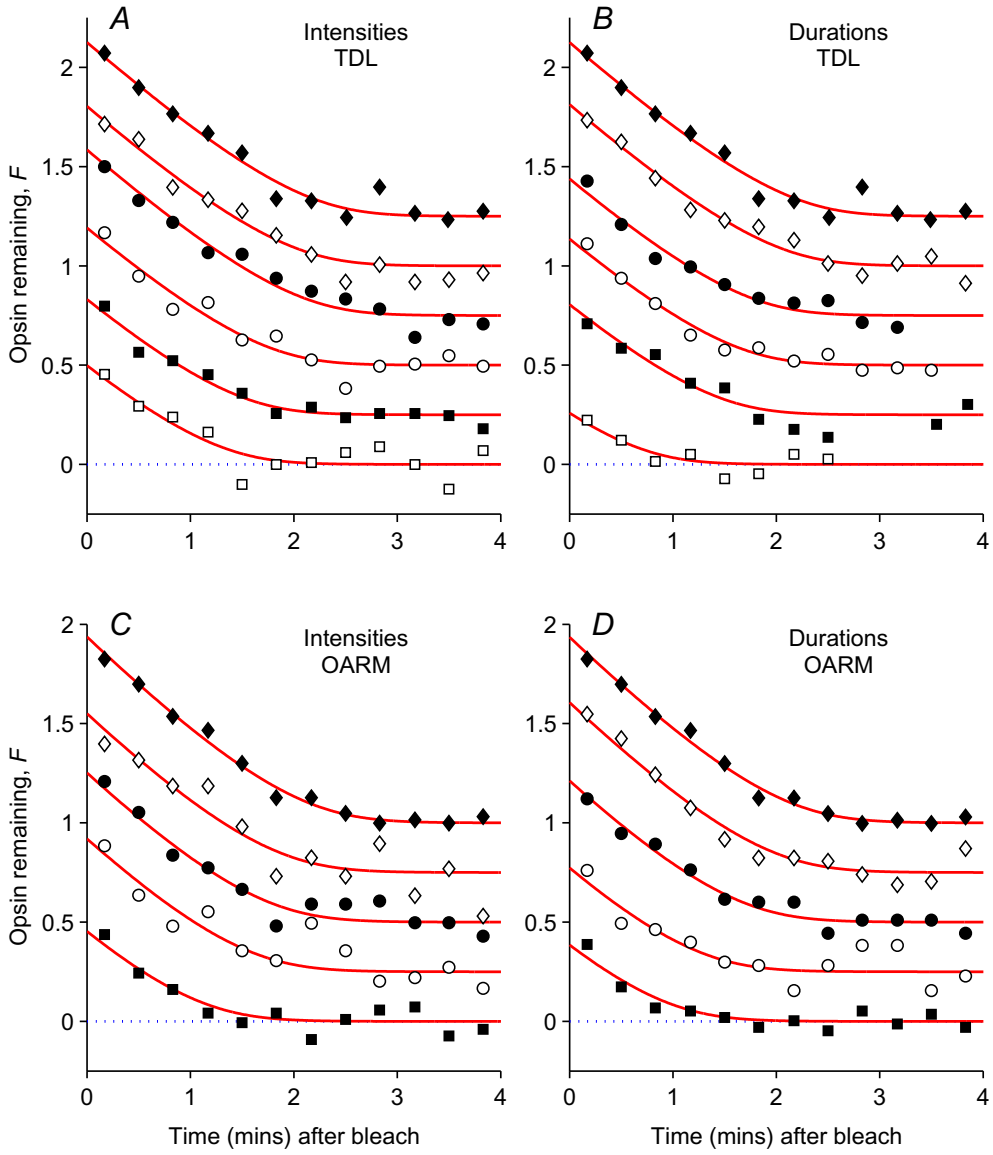

Fig. 5. Post-bleach recovery of opsin level in human cone photoreceptors, measured using the ERG *a*-wave. Results are taken from Fig. 7 of Mahroo and Lamb (2004), where the fractional level of cone pigment was estimated from the amplitudes of ERG responses elicited by dim photopic flashes; here the fractional opsin level is plotted as the complement of their estimated cone pigment level. The upper panels are for subject TDL, and the lower panels are for subject OARM. The left hand column (Intensity) is for exposures of different intensity, with the exposure duration adjusted to be the minimum required to achieve a steady-state bleaching level. The intensities were (from top downwards): 3000, 2000, 1500, 1000, 700, 500 cd m^{-2}, except that subject OARM did not receive the lowest intensity. The right hand column (Durations) is for exposures of different duration to a fixed intensity of 3000 cd m^{-2}; the durations were 60, 40, 20, 15, 10, 5 s, except that subject OARM did not receive the shortest duration. The red curves plot the predictions of the enzymatic model, optimised using $K_2 = 2$. For subject TDL, the fitted parameters were: $K_1 = 0.26, k = 4.2$ min^{-1}, and bleach levels from 26% to 88%, with normalised residual $SS_{resid} = 0.048$. For subject OARM, the fitted parameters were: $K_1 = 0.33, k = 3.7$ min^{-1}, and bleach levels from 39% to 94%, with normalised residual $SS_{resid} = 0.067$. (For interpretation of the references to colour in this figure legend, the reader is referred to the web version of this article.)

the data points is expected to be constant. Where data points have been excluded from the optimisation procedure, this is indicated by blue lines (Figs. 3 and 4B). The residual sum-of-squares error is presented in normalised form, SS_{resid} (defined as residual variance/data variance), so that the R^2 parameter (coefficient of determination) describing the goodness of the fits is simply $R^2 = 1 - SS_{resid}$. As the bleach levels were not known accurately, these were treated as free parameters in the fitting. An exception was made for the near-total bleach in Fig. 3, which was known to be close to 98%; unless some constraint was made to at least one bleach level, the fitting procedure was prone to return fitted bleach levels either greater than 100% or unreasonably small. In preliminary attempts at fitting the enzymatic model, we found that SS_{resid} was only very weakly dependent on the magnitude of either K_1 or K_2 alone (see, for example, the description for Fig. 3 below). Therefore, we chose to fix K_2 while optimising all other parameters. The weakness of this dependence made it unrealistic in practice to choose between the enzymatic and resistive models solely on the basis of the quality of the fitting; we expand upon this notion in Section 4. For the curves shown in Figs. 2–5 we chose the fixed value as $K_2 = 2$; this magnitude was chosen in order to elicit a shape of recovery broadly similar to that for the resistive model (see Appendix A, Fig. 6) while not approaching the limit in which the two models converge ($K_2 \to \infty$).

For the psychophysical dark adaptation results presented in Fig. 3, optimisation of the parameters of the enzymatic model, with

$K_2 = 2$, generated the red traces. For this individual the fitted rate parameter was $k = 0.60\ \text{min}^{-1}$, corresponding to an S2 slope ($= k/\ln 10$) of 0.26 decade min^{-1}. The fitted value of K_1 was $K_1 = 0.50$ which, upon substitution into Eqs. (35) and (36), corresponds to an equivalent K_m in the resistive model of $K_{m,equiv} = 0.21$. The fitted vertical shift was $C_{full} = 4.23\ \log_{10}$ units, indicating that a full complement of free opsin would have raised the threshold of the rod visual system by about 17,000-fold.

For this fit, the normalised residual sum-of-squares error was $SS_{resid} = 0.0208$, corresponding to $R^2 \approx 0.98$. When the value of K_2 for the optimisation was altered, SS_{resid} declined very gently with increasing K_2; it declined by 0.6% for $K_2 = 4$ and by 1.3% for $K_2 \to \infty$. As a check, repetition of the optimisation procedure using the resistive model reproduced the fit obtained using the enzymatic model with $K_2 \to \infty$. The fitted curves for the resistive model (not illustrated) could barely be distinguished by eye from those for the enzymatic model with $K_2 = 2$, which is not surprising in light of the similarity of the respective R^2 values, of 0.97951 and 0.97924. Thus we conclude that the enzymatic and resistive models both provide excellent fits to the experimental data, and that in practice the enzymatic model generates traces so similar to those for the resistive model that it is not practicable to distinguish either model as providing a superior fit to these data.

3.4. Opsin decay in rods measured in patients with fundus albipunctatus

Fundus albipunctatus is a rare form of stationary "night blindness", with predominantly autosomal recessive inheritance. Numerous yellow-white dots are visible in the fundus, and rod dark adaptation and rhodopsin regeneration are both greatly slowed, though serum levels of vitamin A are normal. The disease is caused by mutations in the gene RDH5 encoding the enzyme 11-*cis* retinol dehydrogenase that oxidises the alcohol 11-*cis* retinol to the aldehyde 11-*cis* retinal in the RPE. Hence this disease is expected to disrupt the normal operation of the initial step indicated "Enzyme" in the schematic of Fig. 1.

Fig. 4 illustrates measurements from three *fundus albipunctatus* patients. Panel A plots the deline in opsin level after a full bleach, measured by retinal densitometry in two patients (data from Carr, Ripps, & Siegel, 1974), while panel B plots the recovery of psychophysical threshold following a range of bleaches in another patient (data from Cideciyan et al., 2000). In both panels, the kinetics are far slower than in normal subjects, as typified above by Figs. 2 and 3.

For the patients examined in Fig. 4A using retinal densitometry, the initial rate v of decline in opsin level after a large bleach was approximately 0.009 min^{-1}, an order of magnitude lower than normal. The prediction of the enzymatic model, fitted using $K_2 = 2$ (red trace), provides a good description of the results (normalised residual error $SS_{resid} = 0.016$, i.e. $R^2 \approx 0.98$). Likewise, the resistive model produced a very similar fit (not illustrated), with SS_{resid} within 0.1% of that for the enzymatic model; compared with normal subjects, the value of K_m was reduced $\sim$ 3-fold, to around 0.06.

In Fig. 4B, rod dark adaptation was drastically slowed, taking around 2 h to reach the cone-rod break after a full bleach, and also being very slow after smaller bleaches. The predictions of the enzymatic model, fitted using $K_2 = 2$ (red traces), provide a good description of the experimental results ($SS_{resid} = 0.014, R^2 \approx 0.99$). The blue lines delineate those data points included in the optimisation; thus, measurements were excluded: at early times where a rod plateau was reported by Cideciyan et al. (2000), above the cone threshold, and below the level of a late component of recovery. For these experiments, our initial unconstrained fitting suggested that the values for the bleach levels B were slightly lower that those determined by Cideciyan et al. (2000). We therefore made the assumption that the effective levels of B were reduced from the delivered levels by the presence of a small residual quantity of 11-*cis* retinal dissolved in the outer segments; i.e. $B = B_{delivered} - B_{residual}$. Upon optimisation of the fitting using this constraint, we obtained $B_{residual} = 3.2\%$. The fitted value for the rate constant was $k = 0.093\ \text{min}^{-1}$ (S2 slope ≈ 0.04 decades min^{-1}) around 6-fold lower than normal. Optimisation of the fit of the resistive model generated traces (not illustrated) that were just distinguishable by eye from those for the enzymatic model, and in this case the normalised residual error, SS_{resid}, was 16% worse than for the enzymatic model; the fitted value of the shape parameter was $K_m = 0.092$, about half of normal.

Overall, the results presented in Fig. 4 demonstrate that the post-bleach recovery of opsin level in these three patients with *fundus albipunctatus* is well described by the predictions of both the enzymatic and resistive models, when the rate constant k is reduced by 6- to 10-fold from normal and when the ratio K_1/K_2 (enzymatic model) or K_m (resistive model) is reduced 2- to 3-fold to provide a more abrupt transition from the sloping to horizontal phase in Fig. 4A. Given that the shape parameter K_m in the resistive model is expected to depend on the resistance to diffusion (see Lamb & Pugh, 2004) and not to depend on the properties of any reactions in the RPE, the reduced value for K_m in *fundus albipunctatus* provides a reason for doubting the applicability of the resistive model. Hence, even though the kinetics of post-bleach recovery are explicable by either model, our interpretation of the *fundus albipunctatus* results is that post-bleach recovery is likely to be accounted for not by a resistive mechanism but instead by an enzymatic reaction step, presumably mediated by some other enzyme, with the reaction rate considerably reduced from normal.

3.5. Opsin decay measured in cone photoreceptors for normal human subjects

In comparison with the situation in rods, the regeneration of visual pigment in cones has been examined in relatively few studies, in part because the densitometric measurements tend to be noisier. Because of the paucity of cones in the human retina ($\sim$5% of the number of rods), the amplitude of the absorption signal in reflection densitometry experiments is quite small, and hence the signal-to-noise ratio is poorer than for measurements of rhodopsin in rods.

An alternative method for monitoring cone pigment regeneration in the human eye using measurements of the electroretinogram (ERG) was developed by Mahroo and Lamb (2004), who provided evidence that the amplitude of the ERG *a*-wave response to a dim flash of light was proportional to the level of visual pigment in the cones.

Fig. 5 plots the post-bleach decline in cone opsin level (obtained as the complement of the level of cone visual pigment that they obtained) for a series of bleaching exposures in two normal human subjects (themselves). The predictions of the enzymatic model, fitted for $K_2 = 2$ (red traces), provide a good description of the experimental results for the entire set of exposures for each subject; the normalised residual error was $SS_{resid} = 0.048$ (for TDL) and 0.067 (for OARM), corresponding to $R^2 \approx 0.95$ and 0.93, respectively. The fitted values of the limiting initial slope for cone opsin recovery, of $v = 0.45$ (TDL) and 0.50 (OARM) min^{-1}, were around 5-fold higher than for rod opsin recovery in normal subjects (typically 0.1 min^{-1}). The fitted values of the rate constant, $k = 4.2$ (TDL) and 3.7 (OARM) min^{-1}, for cone opsin recovery were roughly 6-fold higher than for normal rod opsin recovery (e.g. 0.60 min^{-1} in Fig. 3). For the resistive model, the fitted curves

(not illustrated) were barely distinguishable by eye from those for the enzymatic model, with normalised residual errors that were 0.5% worse (for TDL) and 0.4% better (for OARM).

4. Discussion

Our first interpretation of the results presented in Figs. 2–5 is that the enzymatic model for the synthesis of 11-*cis* retinal and the resistive model of restricted diffusional access are each capable of providing a good description of experimental measurements of opsin decline in the living human eye, both for rods and for cones in normal subjects, as well as for rods in the case of the disease *fundus albipunctatus* in which the enzyme RDH5 is compromised. However, as we now discuss, there are a number of reasons for doubting that the resistive model is genuinely applicable.

In the early 1980s it was reported that for the human scotopic (rod) visual system the bleach-induced elevation of threshold, and its subsequent recovery, could be described by rate-limited removal of a bleaching product that weakly mimicked the effects of light (Lamb, 1981). Subsequently, in the mid-1990s, it was shown in animal experiments that the opsin that is produced as a result of bleaching exposures weakly mimics light activation (Cornwall & Fain, 1994), and so opsin became a prime suspect for the source of the threshold elevation during human dark adaptation following bleaching exposures. Then, in the early 2000s, it was proposed that the cause of the rate-limit in the post-bleach removal of opsin might be the existence of some kind of resistive barrier to the flow of 11-*cis* retinal from its site of synthesis in the RPE to its site of consumption in the photoreceptor outer segments (Lamb & Pugh, 2004; Mahroo & Lamb, 2004), and the predictions of that resistive model were shown to be capable of describing the experimental measurements (Lamb & Pugh, 2004).

We contend that, although a resistive model is *capable* of describing the experimental results, there is no experimental evidence that directly supports such a mechanism, and we hold this view despite the claims of two recent studies. In the first of these studies, Frederiksen et al. (2012) employed a chemical analog, 4-hydroxy-11-*cis* retinal that has greater aqueous solubility, and they demonstrated more rapid regeneration of visual pigment. However, after correction of a computational error (Frederiksen et al., 2014), their experimentally measured flux of retinoid was ~2000× smaller than the limiting flux that they calculated theoretically could flow through the resistance of the narrow aqueous gap within the outer segment, indicating that their proposed resistive mechanism would cause negligible resistance in practice. In the second study, Kessler et al. (2014) used early receptor potential (ERP) measurements to extract the time-course of pigment regeneration in the plasma membrane of mouse rods, and they showed that this was faster than the time-course of regeneration of bulk rhodopsin that had been measured in studies a decade earlier in the same strain of mouse. However, as regeneration of bulk rhodopsin was not actually measured in the mice that were studied electrophysiologically, there was no firm evidence that the regeneration kinetics do indeed differ between the surface membrane and the interior membranes.

The recent study of Wang et al. (2014) has shown much faster post-bleach recovery of sensitivity in the same strain of mouse (C57BL/6) that Kessler et al. (2014) used, suggesting that the kinetics of rhodopsin regeneration might vary between batches of animals of notionally the same strain. Accordingly, although there remains a possibility that the recovery of rhodopsin proceeds more slowly in the disc membranes than in the plasma membrane, this has yet to be demonstrated directly, and we do not accept that the experiments of Kessler et al. (2014) provide evidence for a significant resistance to the flow of retinoid from plasma membrane to disc membrane. Furthermore, Wang et al. (2014) additionally examined genetically-modified mouse rods, that had been engineered so as to have access to retinoid from an alternative source within the retina (in the way that cones have). They concluded that the limitation to rhodopsin regeneration in mouse rods arises from a limitation in the *supply* of 11-*cis* retinoid to the rods.

Further evidence casting doubt on the applicability of the resistive model to rod opsin regeneration comes from our own analysis in Fig. 4, for patients with *fundus albipunctatus*, where the optimised fitting indicated that the shape parameter K_m in the resistive model was around half to one-third of the value reported for rod opsin recovery in normal subjects. From Eq. (5) of Lamb and Pugh (2004) this parameter is defined as $K_m = 1/kR$, where k is the bimolecular rate constant (as defined here) and R is the "resistance" to diffusion from the fixed concentration of 11-*cis* retinal to the opsin in the photoreceptors. However, there does not appear to be any obvious reason for expecting a change in this postulated resistance in *fundus albipunctatus* (or indeed in any disease affecting the proteins that resynthesise 11-*cis* retinal in the retinoid cycle). In order to support the resistive model one would need to provide an explanation for the altered K_m that we found in patients with *fundus albipunctatus*.

In the case of cone photoreceptors, the post-bleach regeneration of pigment has previously been shown to be rate-limited (Mahroo & Lamb, 2004), and in Fig. 5 we found that the decline in cone opsin level could again be described well by the predictions of the enzymatic model, in this case with the rate constant k raised by a factor of around 6-fold from that needed for rods in a normal subject. Cones provide another interesting test for the resistive model, because the opsin molecules reside in the surface membrane, rather than in internal disc membranes, so that the resistive bottle-neck from the surface membrane to opsin molecules suggested to apply for rods by Frederiksen et al. (2012) and Kessler et al. (2014) cannot be invoked. Therefore, if the resistive model is to be applicable to cones, then the postulated resistance must be shown to reside elsewhere.

Hence, although the resistive model is capable of accounting for the measurements, there has been no compelling evidence provided for the existence of cellular mechanism(s) that could underlie the resistive model, either for a source of 11-*cis* retinal at fixed concentration, or for a suitable resistance. The most obvious alternative to the resistive model, as a contender for a mechanism limiting the supply of 11-*cis* retinal for the regeneration of visual pigment, is an enzymatic reaction involved in the synthesis of 11-*cis* retinal, as has been suggested either implicitly or explicitly by many studies over the years. Thus, there are clearly-defined molecular mechanisms known for the enzymatic steps involved in the synthesis of 11-*cis* retinaldehyde, that could provide such a limit. Accordingly we presume that it is actually the enzymatic model that provides the cellular basis for the regeneration of rod and cone visual pigments.

Through mathematical analysis of the enzymatic model we have derived an analytical solution for the kinetics of rhodopsin regeneration that it predicts. Our formulation is characterised by three parameters: a bimolecular rate constant k that is shown to specify the rate of opsin's final exponential decline, together with two parameters K_1 and K_2 that characterise the enzyme-assisted reaction that creates 11-*cis* retinal. K_1, defined in Eq. (7), is a scaling constant proportional to the total quantity of enzyme, while K_2, defined in Eq. (8), is the fractional level p of the product P at which half of the enzyme is free and hence available for binding (i.e. not bound as the intermediate form I·E shown in the reaction scheme in Eq. (3)). Our analytical solution for the post-bleach kinetics of decline in opsin level, $F(t)$, is given by Eqs. (24) and (26).

In Figs. 6 and 7 of Appendix A we compare the predictions of the enzymatic and resistive models, for parameter values in the range anticipated to apply for the experimental data; i.e. corresponding to $K_m \approx 0.2$ in the resistive model. In linear and semi-logarithmic coordinates, the shape of the predicted time-course of opsin decline in the two models is qualitatively similar, over a fairly broad range of values for K_2, when K_1 is appropriately constrained. Indeed, in the limit of $K_2 \to \infty$ (when all of the enzyme is bound in the intermediate form) the predictions of the enzymatic model become identical to those of the resistive model.

In Figs. 2 and 3 of the Results section we examined the ability of the enzymatic model to describe experimental measures of post-bleach opsin level for rods in the living human eye, obtained using retinal densitometry (in Fig. 2) or from a subject's visual threshold elevation (in Fig. 3). We found that the predictions provided a good fit to the measurements, with an R^2 value of around 0.98. Likewise, the predictions of the resistive model provided a fit that was closely similar (not illustrated), with almost the same > value. We interpret this finding to indicate that for the enzymatic model to describe normal rod opsin recovery it needs to predict a shape broadly similar to that predicted by the resistive model with $K_m \approx 0.2$, and in practice this means that $K_2 \gtrsim 1$. Because of the variability/noise in the experimental measurements, it is not feasible to extract precise estimates of the parameters K_1 and K_2 in the enzymatic model.

In Fig. 4 we examined the ability of the enzymatic model to describe the decline of opsin level in the human disease *fundus albipunctatus*, in which there is a deficiency in the enzyme 11-*cis* retinol dehydrogenase (RDH5) that catalyses the final step in the synthesis of 11-*cis* retinaldehyde in the retinal pigment epithelium (RPE). We found that the predictions for $F(t)$ provided good descriptions both for the densitometry measurements following a full bleach (Fig. 4A) and also for the psychophysical dark adaptation measurements over a wide range of bleaching levels (Fig. 4B). The lower fitted value of k, compared with normal rod opsin recovery, suggests that an alternative "backup" enzymatic pathway is available when the RDH5 is non-functional, operating at a rate around 6- to 10-fold lower than normal.

Putting these results together, we conclude that the enzymatic model is capable of accounting for the observed post-bleach regeneration of visual pigment in human subjects under all the circumstances that we have examined. And, in contrast to the case of the resistive model, we know of no reason for doubting its applicability as the cellular mechanism underlying the rate-limited regeneration of visual pigment.

In our description of the enzymatic model (see Fig. 1) we have portrayed the reaction explicitly in terms of the conversion of 11-*cis* retinol (the alcohol) into 11-*cis* retinal (the aldehyde), which is normally mediated by the enzyme RDH5 (11-*cis* retinol dehydrogenase). This conversion step would seem likely to contribute to the rate limit in normal human dark adaptation recovery, and it would seem bound to contribute a limitation when the reaction becomes slow, for example because of a problem with the RDH5 enzyme. However, in certain diseases, or in the dietary condition of vitamin A deficiency, or in other species (such as mouse), it is entirely plausible that other reaction steps could instead become rate-limiting. For example, in certain strains of mouse (such as C57BL6) the enzyme RPE65 (isomerohydrolase) that creates 11-*cis* retinol (the alcohol) exhibits far lower activity than in human, so that it might then be appropriate to ignore the subsequent RDH5 step. In such a case it would seem likely that the same analysis as presented here would apply, though the substrate S and product P of the enzymatic reaction would not correspond to those specified in this paper.

5. Competing interests

The authors declare that they have no competing interests.

6. Author contributions

T.D.L. and R.M.C. conceived the overall goals of the work. R.M.C. derived the analytical solution for the kinetics. ADP wrote and tested the Maple code, and carried out numerical comparisons. T.D.L. wrote the manuscript and created the Figures. All authors read and approved the final manuscript.

Acknowledgements

This work was supported in part by Australian Research Council Grant CE0561903 (TDL), by NSERC, and by the Distinguished University Professorship awarded to R.M.C. by the University of Western Ontario.

Appendix A. Analytical solutions for the equations

Here, we derive an analytical solution for the kinetics of rhodopsin regeneration, in the case where 11-*cis* retinoid is produced by an enzymatic reaction of the kind illustrated in Fig. 1. Then we investigate the dependence of the predicted rate on the values of the reaction parameters.

A.1. Solution for 11-cis retinal concentration

For the case of a fixed concentration of substrate, Lamb and Pugh (2006) analysed the forward and reverse reactions of the enzymatic scheme (illustrated as Eq. (3) above), and expressed the net rate of product formation r in terms of the absolute concentration P of product as their Eq. A6. Upon substitution using their Eq. A5, that expression can be written as

$$r(t) = k_{IS} E_{tot} \frac{1 - \frac{P(t)}{P_0}}{\frac{K_P}{P_0} + \frac{K_P}{KK_S} + \frac{P(t)}{P_0}}. \tag{5}$$

Apart from $P(t)$, all of the terms on the right hand side are constants. P_0 is the absolute concentration of product that elicits zero net flux, so that when $P < P_0$ the net flux is in the forward direction and product is generated; as there is no other source of 11-*cis* retinal in the RPE/retina, there should never be net flow in the reverse direction and so we should always have $P \leqslant P_0$. P_0 represents the resting dark-adapted concentration of P, and henceforth we will refer to the product concentration only in terms of its fractional level, $p(t) = P(t)/P_0$. For definitions of the remaining parameters, see Lamb and Pugh (2006).

Applying the quasi-steady state relation Eq. (4), we equate Eqs. (2) and (5), to obtain

$$k_{IS} E_{tot} \frac{1 - p(t)}{\frac{K_P}{P_0} + \frac{K_P}{KK_S} + p(t)} = k p(t) F(t). \tag{6}$$

To simplify our notation, it is convenient to make the substitutions

$$K_1 = \frac{k_{IS} E_{tot}}{k}, \tag{7}$$

$$K_2 = \frac{K_P}{P_0} + \frac{K_P}{KK_S} \tag{8}$$

whereupon Eq. (6) becomes

$$K_1 \frac{1 - p(t)}{K_2 + p(t)} = p(t) F(t). \tag{9}$$

Interestingly, the term $1/(K_2+p)$ in this equation represents the *free* fraction of enzyme E, that is not bound as the intermediate form indicated "I·E" in the reaction scheme, but is instead available for binding; see Eq. A3 in Lamb and Pugh (2006). Hence K_2 represents the level of p at which half the enzyme would be free.

Next we denote

$$\eta(t) = \frac{1}{F(t)}, \tag{10}$$

whereupon Eq. (9) can be rearranged as

$$p^2 + (K_1\eta + K_2)p - K_1\eta = 0. \tag{11}$$

This quadratic has two possible solutions

$$p_{1,2} = \frac{-(K_1\eta + K_2) \pm \sqrt{(K_1\eta + K_2)^2 + 4K_1\eta}}{2}. \tag{12}$$

At a later stage we will use the solution p_2 (with the positive square root) in just this form, but for now there are advantages to expressing p_2 in an alternative form. The product $p_1 p_2$ of the two roots is $-K_1\eta$, so we may write $p_2 = -K_1\eta/p_1$. Using the negative square root for p_1, matching the sign of $-(K_1\eta + K_2)$, gives us the following alternative expression for p_2:

$$p_2 = \frac{2K_1\eta}{K_1\eta + K_2 + \sqrt{(K_1\eta + K_2)^2 + 4K_1\eta}}. \tag{13}$$

Notice that as $F(t) \to 0, \eta \to \infty$ and Eq. (12) shows that $p_1 \to -\infty$, which is unphysical. On the other hand, Eq. (13) shows that $p_2 \to 1$ from below, which conforms with the situation being modelled. Therefore, we choose only p_2.

If we know the fractional opsin level, F, then to obtain the corresponding fractional level of 11-*cis* retinal, p, we simply calculate p_2 using either Eqs. (12) or (13).

A.2. Solution for kinetics of rhodopsin regeneration

We now solve for the time-course $F(t)$ corresponding to our initial condition $F = B$ at $t = 0$. From the right-hand equality in Eq. (2), we have $dF/dt = -kp(t)F(t)$, which implies

$$\frac{d}{dt}\eta(t) = \frac{d}{dt}\left(\frac{1}{F(t)}\right) = -\frac{1}{F^2(t)}\frac{d}{dt}F(t) \tag{14}$$

$$= -\eta^2\left(-kp\frac{1}{\eta}\right) \tag{15}$$

$$= kp\eta(t). \tag{16}$$

This gives us two differential equations, one for each choice of the sign of the square root in Eq. (12). Again, we use only p_2, so that we have

$$\frac{d\eta}{dt} = kp_2\eta(t) \tag{17}$$

and we can usefully make some further gatherings and scalings. By putting

$$u(t) = K_1\eta(t), \tag{18}$$

and multiplying Eq. (17) by K_1, we get

$$\frac{du}{dt} = kp_2 u. \tag{19}$$

We now change the time-scale to

$$T = kt \tag{20}$$

so that Eq. (19) becomes

$$\frac{du}{dT} = p_2 u. \tag{21}$$

Substituting for p_2 from Eq. (13), we obtain

$$\frac{du}{dT} = \frac{2u}{u + K_2 + \sqrt{(u+K_2)^2 + 4u}}u, \tag{22}$$

which can be rewritten further as

$$\frac{u + K_2 + \sqrt{(u+K_2)^2 + 4u}}{2u^2}du = dT. \tag{23}$$

At this point, Maple™ (Maple 16, Maplesoft, a division of Waterloo Maple Inc., Waterloo, Ontario) can do the integral that arises on integrating both sides, and the answer can be massaged so that it contains only real quantities. Let us denote

$$G(u) = \frac{1}{2}\left[\ln(u) - \frac{K_2+2}{K_2}\ln\left(K_2 + 2 + K_2\frac{K_2+\sqrt{\Delta}}{u}\right) + \ln\left(K_2 + 2 + u + \sqrt{\Delta}\right) - \frac{K_2+\sqrt{\Delta}}{u}\right], \tag{24}$$

where

$$\Delta = (u+K_2)^2 + 4u$$

is the discriminant of the quadratic. For $u \geqslant 0$ this discriminant is always positive, and so the expressions in the square roots are always real. Maple then shows that Eq. (23) integrates to

$$G(u(T)) - G(u(T_0)) = T - T_0. \tag{25}$$

Our initial condition, at $t = 0$, is $F(0) = B$, where B is the fractional bleach, so we also have $u(0) = K_1/B$, as well as $T = 0$. Accordingly, we may rewrite Eq. (25) in terms of t as

$$t = \left[G(u) - G\left(\frac{K_1}{B}\right)\right]\Big/k. \tag{26}$$

A.3. Application of the equations

From the equations above, we see that this analysis provides an inverse approach for evaluating the time-course $F(t)$ of opsin decay. First, for an appropriate range of values of F, we evaluate $u = K_1/F$; next, we substitute the resulting u into Eq. (24) to obtain $G(u)$; finally, we use Eq. (26) to evaluate t.

In order to aid selection of appropriate values for the parameters K_1 and K_2, for comparison with experimental results, we now investigate some cases of interest, including the initial rate of recovery after a total bleach and the recovery at late times.

A.3.1. Initial rate of rhodopsin regeneration after a total bleach

Of particular interest is the situation at the extinction of a total bleach, $B = 1$, when all the rhodopsin has been converted to opsin, so that $Rh = 0$ and $F = 1$. We will denote the induced concentration of product p at this instant as p_0, which we obtain from Eq. (12) using the positive sign of the square root as

$$p_0 = \frac{1}{2}\left(\sqrt{(K_1+K_2)^2 + 4K_1} - (K_1+K_2)\right). \tag{27}$$

In accordance with Lamb and Pugh (2004) and Mahroo and Lamb (2004), we introduce the symbol v to denote the initial rate of rhodopsin regeneration (and of opsin decay) following a total bleach, which we obtain from Eq. (2) as

$$v = \left.\frac{dRh}{dt}\right|_{Rh=0} = -\left.\frac{dF}{dt}\right|_{F=1} = kp_0. \tag{28}$$

In order to compare the resistive and enzymatic models, it is convenient to constrain this initial rate v of regeneration following a total bleach to be equal in the two models. For the resistive model, Lamb and Pugh (2004) derived the initial rate as

$$v = k\frac{K_m}{1+K_m}. \tag{29}$$

Hence, to equate the initial rates in the two models, we require

$$p_0 = \frac{K_m}{1+K_m}. \tag{30}$$

First, we rearrange Eq. (27) to give

$$K_1 = \frac{p_0(p_0+K_2)}{1-p_0}, \tag{31}$$

and then we substitute from Eq. (30) to yield

$$K_1 = K_m\left(K_2 + \frac{K_m}{1+K_m}\right). \tag{32}$$

When K_1 is constrained according to this expression, the enzymatic and resistive models will exhibit a common initial rate v of regeneration following a total bleach.

A.3.2. Common behaviour in the limit of large K_2

In the limit as $K_2 \to \infty$ (when the free fraction of enzyme becomes negligible) the solution for the enzymatic model approaches that for the resistive model, given in Eq. (1). This occurs because in this limit the denominator on the right hand side of Eq. (5) loses its dependence on p, so that Eq. (5) reduces to the form $r \propto (1-p)$, exactly as in the resistive model. In this limit, Eq. (32) reduces to

$$\frac{K_1}{K_2} = K_m. \tag{33}$$

Hence, as $K_2 \to \infty$ with K_1 constrained in this way, the solutions for the enzymatic and resistive models become identical.

A.3.3. Limiting behaviour at late times

At late times, the final tail of recovery in both models is an exponential decay, $\exp(-kt)$, and we can write

$$F(t)|_{t\to\infty} \to \exp\left(k(t_{shift}-t)\right) \tag{34}$$

where t_{shift} is a model-dependent time shift that we will denote as t_{res} and t_{enz}, respectively for the resistive and enzymatic models.

For the enzymatic model, examination of Eqs. (24) and (26) yields the time shift as

$$t_{enz} = \frac{1}{2}\left[\ln K_1 + \frac{K_2+2}{K_2}\ln\left(\frac{K_2+2+\frac{K_2}{K_1}\left(K_2+\sqrt{\Delta_0}\right)}{2+2K_2}\right) - \ln\left(K_1+K_2+2+\sqrt{\Delta_0}\right) + \frac{K_2+\sqrt{\Delta_0}}{K_1} + \ln 2 - 1\right] \tag{35}$$

with

$$\Delta_0 = (K_1+K_2)^2 + 4K_1.$$

For the resistive model, Eq. (1) instead yields the much simpler form for the time shift as

$$t_{res} = \frac{1}{K_m}. \tag{36}$$

A.4. Form of predicted decline, and comparison between models

We now examine the predictions of the two models. Although there is insufficient information to specify unique values for K_1 and K_2, we do know that in the resistive model a value of $K_m \approx 0.2$ provides an adequate description for several sets of experimental data (Lamb & Pugh, 2004). Therefore we will begin by comparing the predictions of the enzymatic model with those of the resistive model when $K_m = 0.2$, and we will do so both in linear and in semi-logarithmic coordinates. In the enzymatic model we will allow K_2 to range from very small to very large, and, for convenience, we will constrain K_1 to provide common behaviour between the two models, either at early times (in the linear plots) or at late times (in the semi-logarithmic plots).

A.4.1. Predicted kinetics in linear coordinates

The full-bleach predictions for the enzymatic model are compared with those for the resistive model in linear coordinates in Fig. 6; for all traces the initial slope (from $F = 1$) has been constrained to be common. For the resistive model, the grey traces are the predictions of Eq. (1) for a range of values of K_m. The time axis is correct for $K_m = 0.2$, but for the other grey traces this time axis has been further scaled so as to yield a common initial slope; from Eq. (29) the required further time scaling is $K_m/(1+K_m)$. For the enzymatic model, the coloured traces are the predictions of Eqs. (24) and (26) for a range of values of K_2, from very small to very large. In each case, K_1 has been constrained according to Eq. (32) with $K_m = 0.2$, so as to give the same initial slope as for the resistive model.

Note that in Fig. 6 the entire set of curves for the enzymatic model broadly resembles a subset of those for the resistive model. Indeed, the red curve for the enzymatic model with large K_2 hides the grey curve for the resistive model with $K_m = 0.2$ (because that is the value of K_m that was used in the constraint). Similarly, the cyan curve for $K_2 = 0.3$ is broadly similar to the grey curve for $K_m = 0.4$.

A.4.2. Predicted kinetics in semi-logarithmic coordinates

The full-bleach predictions for the enzymatic model are plotted in semi-logarithmic coordinates in Fig. 7, for the same set of values of K_2, though with K_1 now constrained so as to provide a common lateral shift of the final exponential decay at late times. The uppermost (red) curve is for a large value of K_2, and it superimposes a

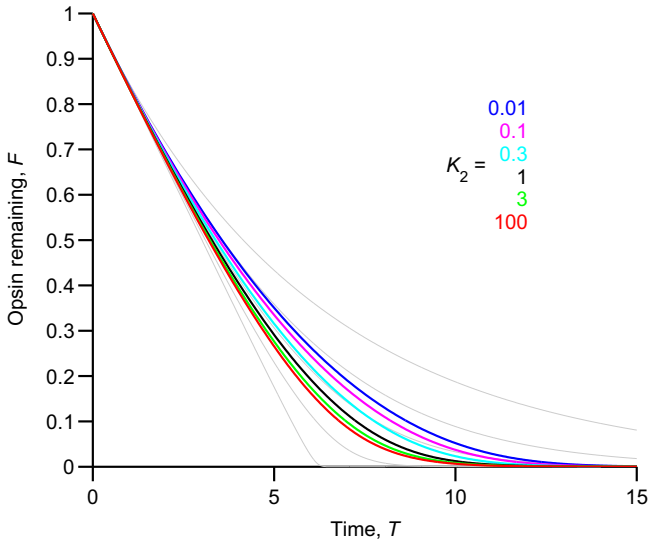

Fig. 6. Comparison of predicted opsin decay kinetics for the resistive and enzymatic models, in linear coordinates. The predictions of the analytical solutions for the resistive and enzymatic models are compared, in linear coordinates, against scaled time $T = kt$, following a total bleach ($B = 1$). To aid comparison, the parameters in the two models have been constrained so as to yield a common initial slope for all traces. Resistive model (grey traces): K_m increases from bottom upwards: 0.05, 0.1, 0.2, 0.4, 1; however, the grey trace for $K_m = 0.2$ is obscured by the red trace (see below). The time axis is correct for $K_m = 0.2$, but has been scaled relative to this by $K_m/(1+K_m)$ for other values. Enzymatic model: K_2 increases from top downwards: 0.01 (blue), 0.1 (magenta), 0.3 (cyan), 1 (black), 3 (green), 100 (red). K_1 has been constrained according to Eq. (32) with $K_m = 0.2$. (For interpretation of the references to colour in this figure legend, the reader is referred to the web version of this article.)

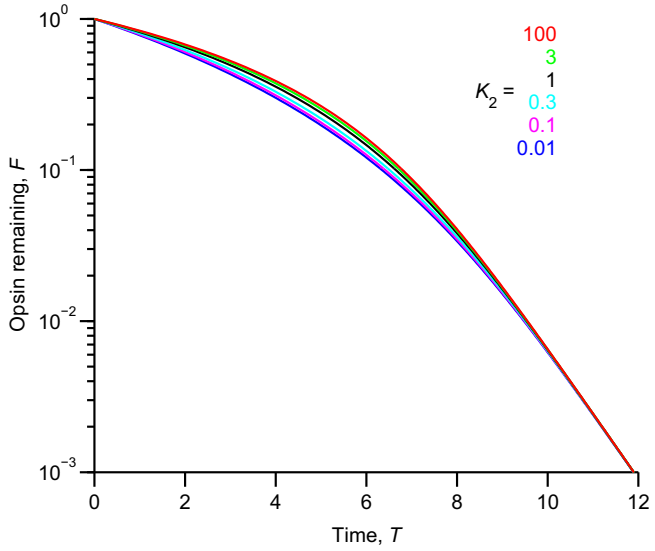

Fig. 7. Predicted opsin decay kinetics for the enzymatic model, in semi-logarithmic coordinates. The predictions of the analytical solution for the enzymatic model are shown, in semi-logarithmic coordinates, against scaled time $T = kt$, following a total bleach ($B = 1$). K_2 increases from bottom upwards: 0.01 (blue), 0.1 (magenta), 0.3 (cyan), 1 (black), 3 (green), 100 (red). K_1 has been constrained by equating Eqs. (35) and (36) for $K_m = 0.2$, so that the lateral shift to the final tail is common. The uppermost trace (red), with $K_2 = 100$, completely obscures a grey trace for the resistive model with $K_m = 0.2$. (For interpretation of the references to colour in this figure legend, the reader is referred to the web version of this article.)

grey trace for the resistive model, with $K_m = 0.2$ (which is therefore not visible). In these coordinates, the shape of the recovery is only weakly dependent on K_2, so that even the black trace, with $K_2 = 1$, is quite similar in shape to the red trace with K_2 large.

References

Campbell, F. W., & Rushton, W. A. H. (1955). Measurement of the scotopic pigment in the living human eye. *Journal of Physiology, 130*, 131–147.

Carr, R., Ripps, H., & Siegel, I. (1974). Visual pigment kinetics and adaptation in *fundus albipunctatus*. *Documenta Ophthalmologica Proceedings Series, 4*, 193–204.

Cideciyan, A., Haeseleer, F., Fariss, R., Aleman, T., Jang, G.-F., Verlinde, C., Marmor, M., Jacobson, S., & Palczewski, K. (2000). Rod and cone visual cycle consequences of a null mutation in the 11-cis-retinol dehydrogenase gene in man. *Visual Neuroscience, 17*, 667–678.

Corless, R. M., Gonnet, G. H., Hare, D. E., Jeffrey, D. J., & Knuth, D. E. (1996). On the Lambert W function. *Advances in Computational Mathematics, 5*, 329–359.

Cornwall, M. C., & Fain, G. L. (1994). Bleached pigment activates transduction in isolated rods of the salamander retina. *Journal of Physiology, 480*, 261–279.

Frederiksen, R., Boyer, N. P., Nickle, B., Chakrabarti, K. S., Koutalos, Y., Crouch, R. K., Oprian, D., & Cornwall, M. C. (2012). Low aqueous solubility of 11-cis-retinal limits the rate of pigment formation and dark adaptation in salamander rods. *Journal of General Physiology, 139*, 493–505.

Frederiksen, R., Boyer, N. P., Nickle, B., Chakrabarti, K. S., Koutalos, Y., Crouch, R. K., Oprian, D., & Cornwall, M. C. (2014). Correction: low aqueous solubility of 11-cis-retinal limits the rate of pigment formation and dark adaptation in salamander rods. *Journal of General Physiology, 144*, 487.

Kessler, C., Tillman, M., Burns, M. E., & Pugh, E. N. Jr, (2014). Rhodopsin in the rod surface membrane regenerates more rapidly than bulk rhodopsin in the disc membranes in vivo. *Journal of Physiology, 592*, 2785–2797.

Kiser, P. D., Golczak, M., & Palczewski, K. (2013). Chemistry of the retinoid (visual) cycle. *Chemical Reviews, 114*, 194–232.

Lamb, T. D. (1981). The involvement of rod photoreceptors in dark adaptation. *Vision Research, 21*, 1773–1782.

Lamb, T. D., & Pugh, E. N. Jr, (2004). Dark adaptation and the retinoid cycle of vision. *Progress in Retinal and Eye Research, 23*, 307–380.

Lamb, T. D., & Pugh, E. N. Jr., (2006). Phototransduction, dark adaptation, and rhodopsin regeneration: The Proctor Lecture. *Investigative Ophthalmology and Visual Science, 47*, 5138–5152.

Mahroo, O. A. R., & Lamb, T. D. (2004). Recovery of the human photopic electroretinogram after bleaching exposures: estimation of pigment regeneration kinetics. *Journal of Physiology, 554*, 417–431.

Morgan, J. I. W., & Pugh, E. N. Jr, (2013). Scanning laser ophthalmoscope measurement of local fundus reflectance and autofluorescence changes arising from rhodopsin bleaching and regeneration. *Investigative Ophthalmology and Visual Science, 54*, 2048–2059.

Pugh, E. N. Jr, (1975). Rushton's paradox: rod dark adaptation after flash photolysis. *Journal of Physiology, 248*, 413–431.

Reuter, T. (2011). Fifty years of dark adaptation 1961–2011. *Vision Research, 51*, 2243–2262.

Rushton, W. A. H., & Powell, D. S. (1972). The rhodopsin content and the visual threshold of human rods. *Vision Research, 12*, 1073–1082.

van de Kraats, J., Berendschot, T. T. J. M., & van Norren, D. (1996). The pathways of light measured in fundus reflectometry. *Vision Research, 36*, 2229–2247.

Wang, J.-S., Nymark, S., Frederiksen, R., Estevez, M. E., Shen, S. Q., Corbo, J. C., Cornwall, M. C., & Kefalov, V. J. (2014). Chromophore supply rate-limits mammalian photoreceptor dark adaptation. *Journal of Neuroscience, 34*, 11212–11221.